Supporting Information for

Preferential Mitochondrial Localization of a Goniothalamin Fluorescent Derivative

Ismael Raitz,[†] Roberto Y. de Souza Filho,[§] Lorena P. de Andrade,[§] Jose R. Correa,[*,‖] Brenno A. D. Neto,[*,§] and Ronaldo A. Pilli[*,†,‡]

[†]Institute of Chemistry, University of Campinas, Cidade Universitária Zeferino Vaz, 13083-970 Campinas, SP, Brazil. Email: pilli@iqm.unicamp.br

[‡]Obesity and Comorbidities Research Center, University of Campinas, Cidade Universitária Zeferino Vaz, 13083-862 Campinas, SP, Brazil

[§]Laboratory of Medicinal and Technological Chemistry, Institute of Chemistry, University of Brasília, Campus Universitário Darcy Ribeiro, 70904-970 Brasília, DF, Brazil. Email: brenno.ipi@gmail.com

[‖]Laboratory of Microscopy and Microanalysis, Institute of Biological Sciences, University of Brasília, Campus Universitário Darcy Ribeiro, 70910-900 Brasília, DF, Brazil. E-mail: correa@unb.br

Summary

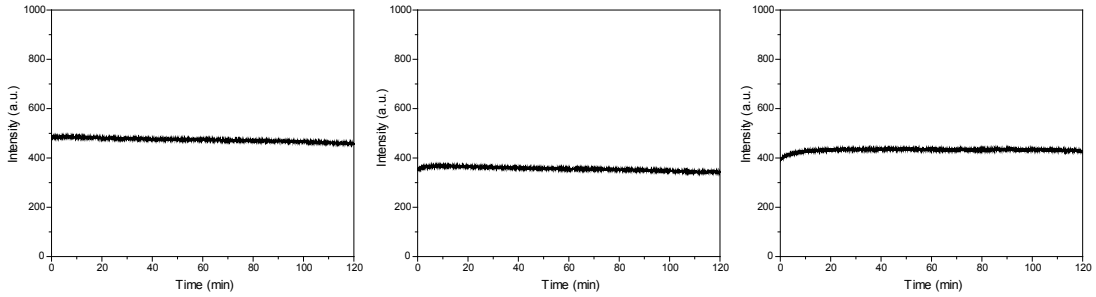

Figure S1. Photostability of BTD-GTN (**1**) acquired at room temperature upon excitation at 405, 366 and 254 nm (respectively) while monitoring the emission at 558 nm. Time-dependence of photoluminescence intensity was carried out with a Xe lamp (400 W).

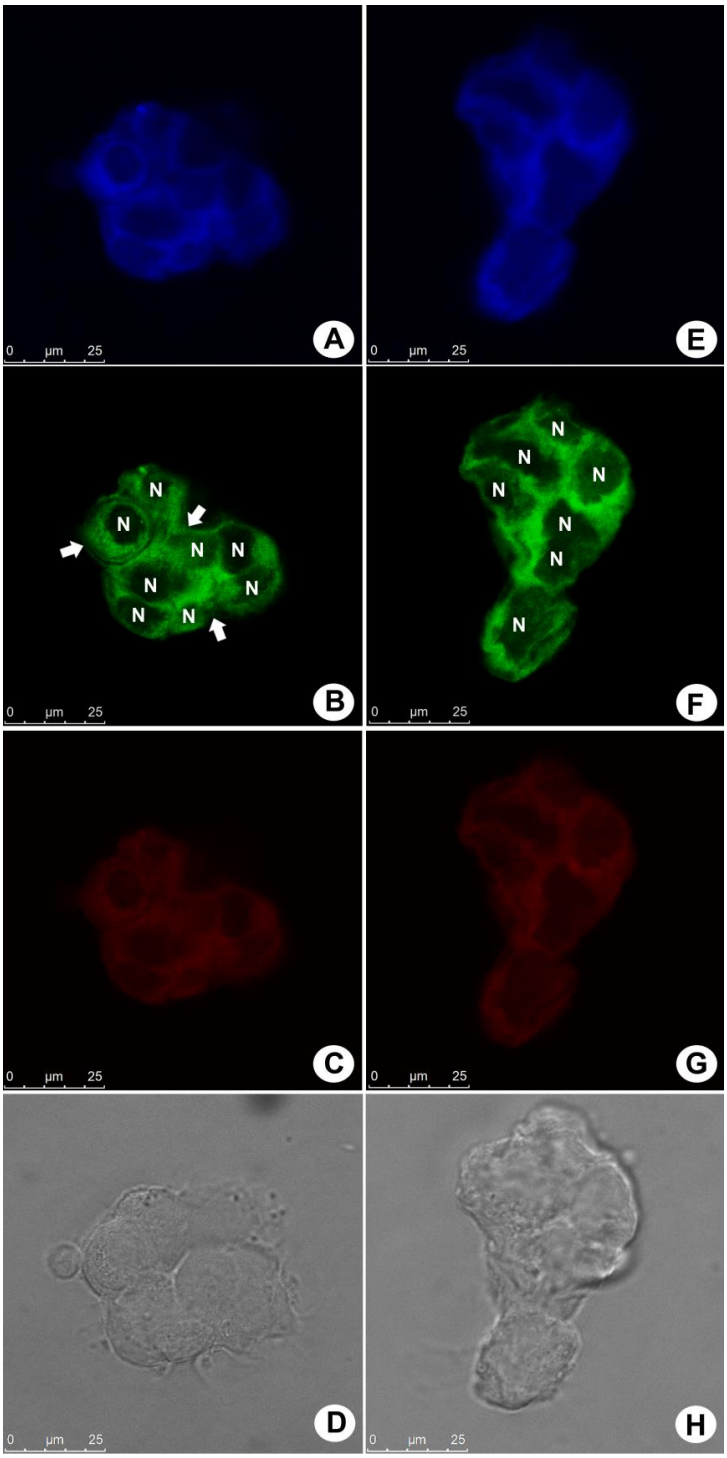

Figure S2. Fluorescent profile of A549 (human lung carcinoma) cells treated with BTD-GTN (**1**) visualised at the blue, green and red channels. Images (A), (B), (C) and (D) show live cells whereas (E), (F), (G) and (H) show fixed cells. (D) and (H) show the morphological aspects of the samples by phase contrast microscopy. Arrows show the cytoplasm distribution of BTD-GTN (**1**) and the nuclei are showed as black voids identified by "N" letters. Reference scale bar 25 µm.

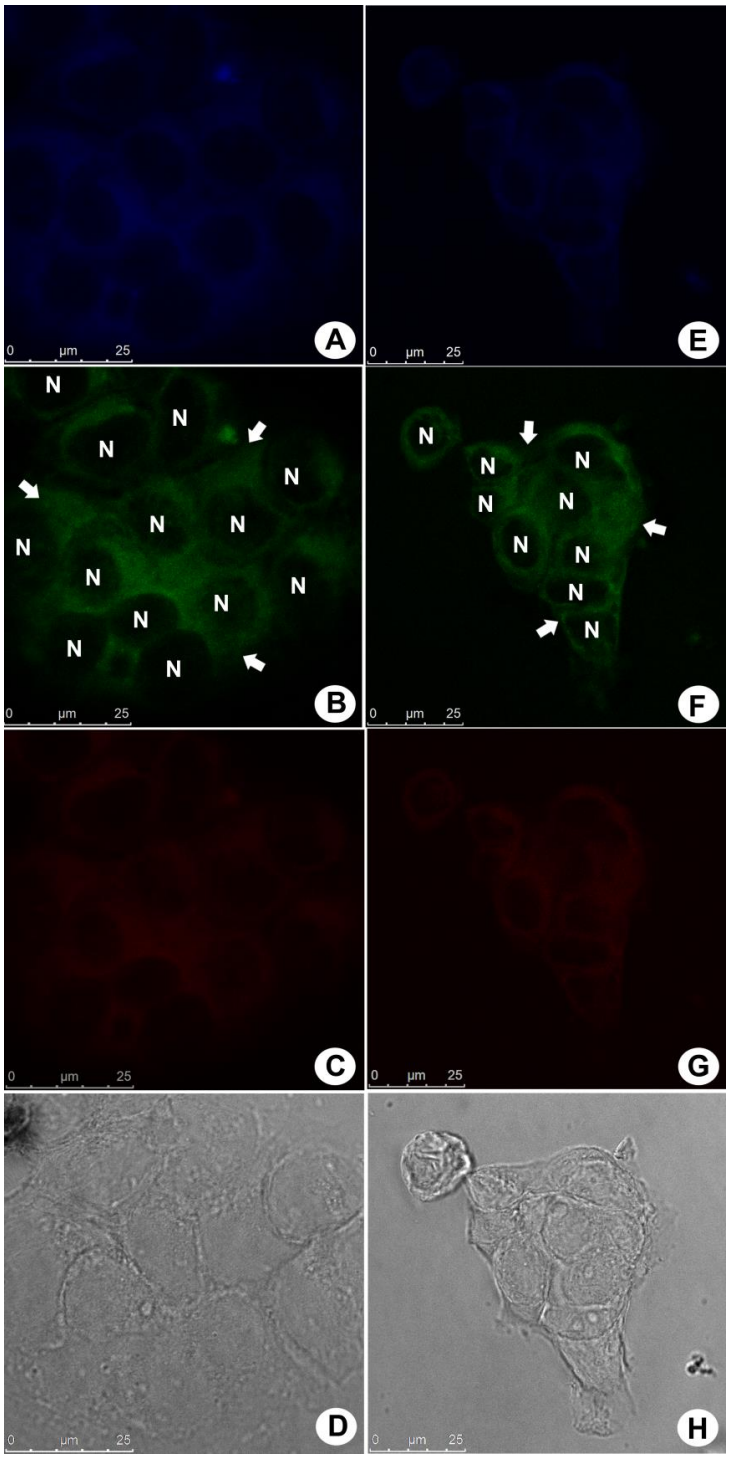

Figure S3. Fluorescent profile of MCF-7 (breast cancer cell line) cells treated with BTD-GTN (**1**) visualised at the blue, green and red channels. Images (A), (B), (C) and (D) show live cells whereas (E), (F), (G) and (H) show fixed cells. (D) and (H) show the morphological aspects of the samples by phase contrast microscopy. Arrows show the cytoplasm distribution of BTD-GTN (**1**) and the nuclei are showed as black voids identified by "N" letters. Reference scale bar 25 µm.

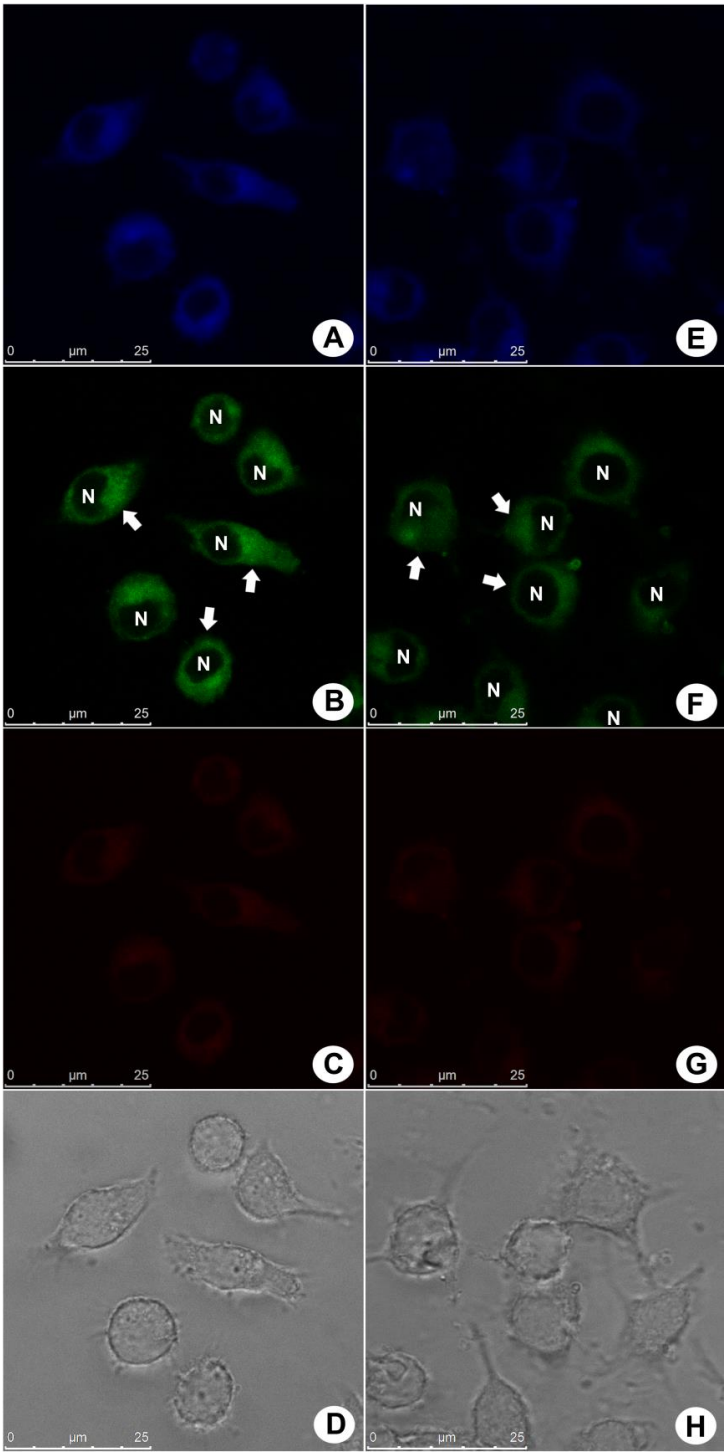

Figure S4. Fluorescent profile of RAW 264.7 (murine macrophage cell line) cells treated with BTD-GTN (**1**) visualised at the blue, green and red channels. Images (A), (B), (C) and (D) show live cells whereas (E), (F), (G) and (H) show fixed cells. (D) and (H) show the morphological aspects of the samples by phase contrast microscopy. Arrows show the cytoplasm distribution of BTD-GTN (**1**) and the nuclei are shown as black voids identified by "N" letters. Reference scale bar = 25 µm.

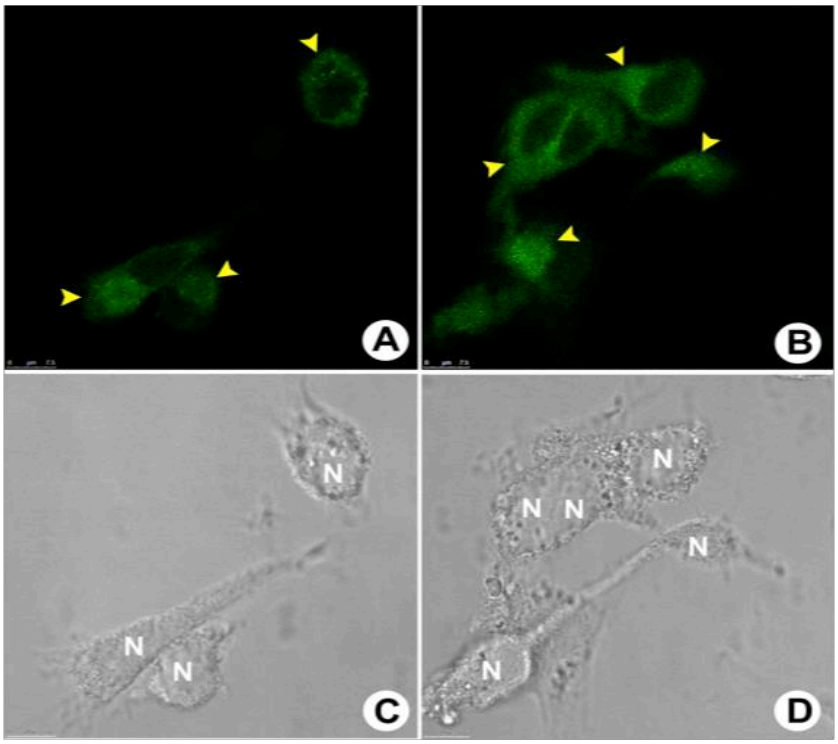

Figure S5. BTD-GTN (**1**) and Rhodamine 1,2,3 staining profile. The images A and B show the cytoplasmic distribution of fluorescence signal. The yellow arrowheads indicate the perinuclear accumulation for both markers. Images C and D show the normal morphological aspects of the cell samples by phase contrast microscopy. The nuclei are indicating by “N" letters. Reference scale bar = 7.5 μm.

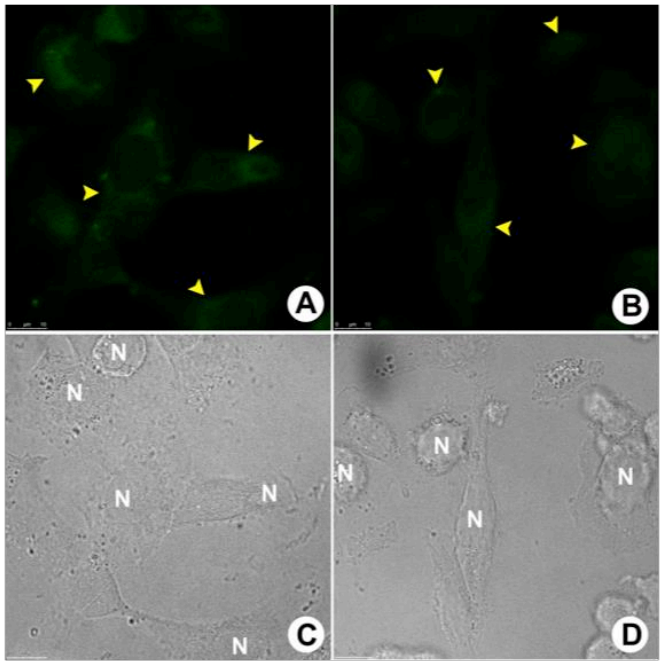

Figure S6. Fluorescence dislodge assay (GTN x BTD-GTN). Image A shows the intensity of fluorescence emission from control sample incubated only with BTD-GTN (**1**). Image B shows the intensity of fluorescence emission from sample pre-incubated with GTN solution at 2.5 μM, followed by incubation with BTD-GTN (**1**) solution 10 μM. Images C and D show the normal morphological aspects of the cell samples by phase contrast microscopy. The cell nuclei are indicated by "N" letters. Reference scale bar = 10 μm.

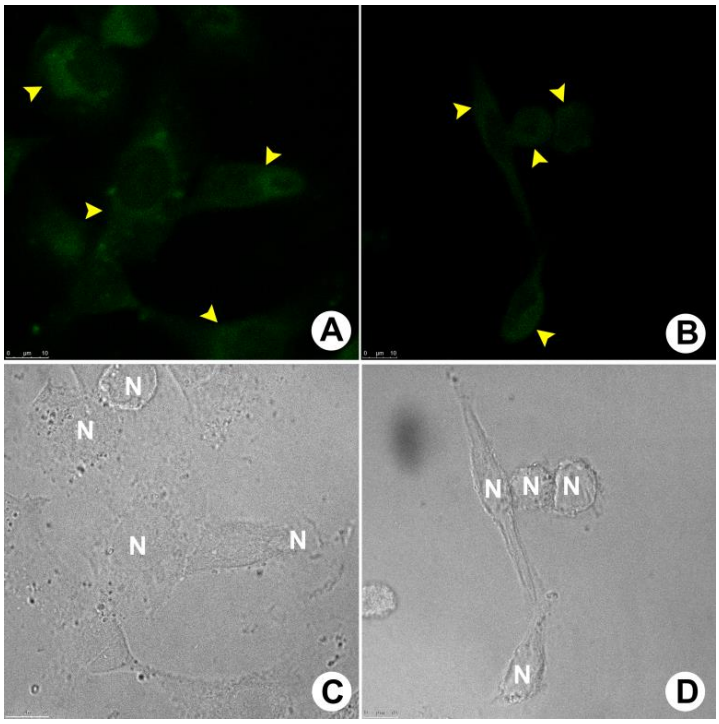

Figure S7. Fluorescence dislodge assay (GTN x BTD-GTN). Image A shows the intensity of fluorescence emission from control sample incubated only with BTD-GTN (**1**). Image B shows the intensity of fluorescence emission from sample pre-incubated with GTN solution at 5 μM, followed by incubation with BTD-GTN (**1**) solution 10 μM. Images C and D show the normal morphological aspects of the cell samples by phase contrast microscopy. The cell nuclei are indicated by “N" letters. Reference scale bar = 10 μm.

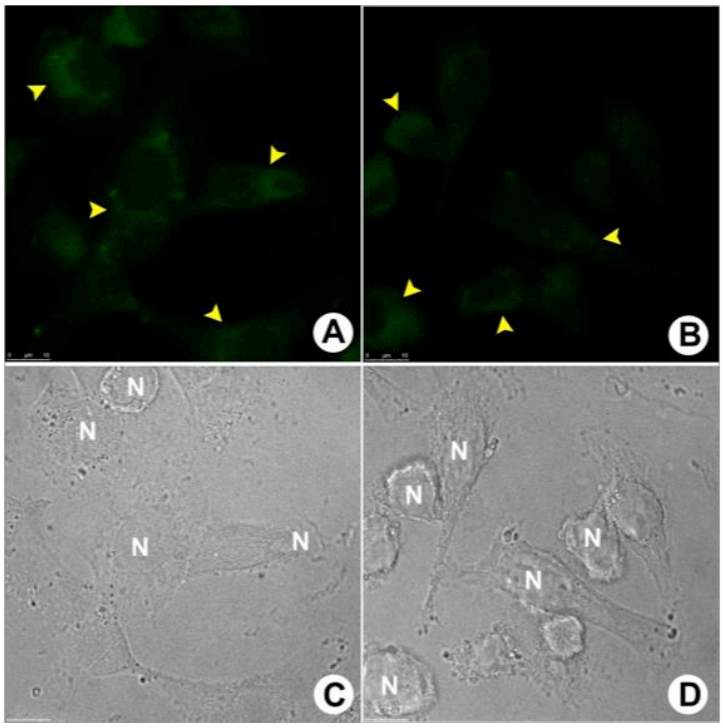

Figure S8. Fluorescence dislodge assay (GTN x BTD-GTN). Image A shows the intensity of fluorescence emission from control sample incubated only with BTD-GTN (**1**). Image B shows the intensity of fluorescence emission from sample pre-incubated with GTN solution at 7.5 μM, followed by incubation with BTD-GTN (**1**) 10 μM solution. Images C and D show the normal morphological aspects of the cell samples by phase contrast microscopy. The cell nuclei are indicated by "N" letters. Reference scale bar = 10 μm.

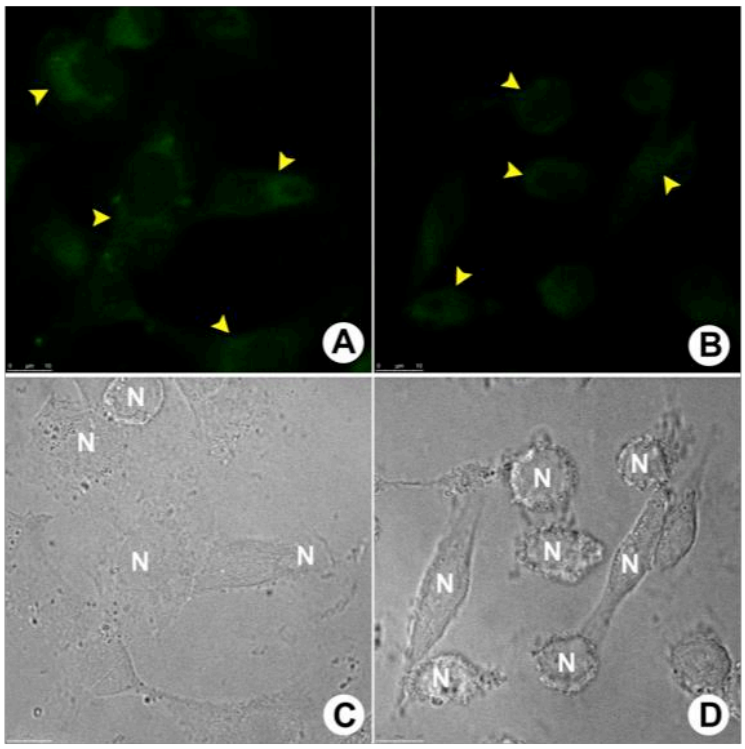

Figure S9. Fluorescence dislodge assay (GTN x BTD-GTN). The images A shows the intensity of fluorescence emission from control sample incubated only with BTD-GTN. The image B shows the intensity of fluorescence emission from sample pre-incubated with GTN solution at 10 μM follow incubation with BTD-GTN solution 10 μM. Images C and D show the normal morphological aspects of the cell samples by phase contrast microscopy. The cells nuclei are indicating by "N" letters. Reference scale bar = 10 μm.

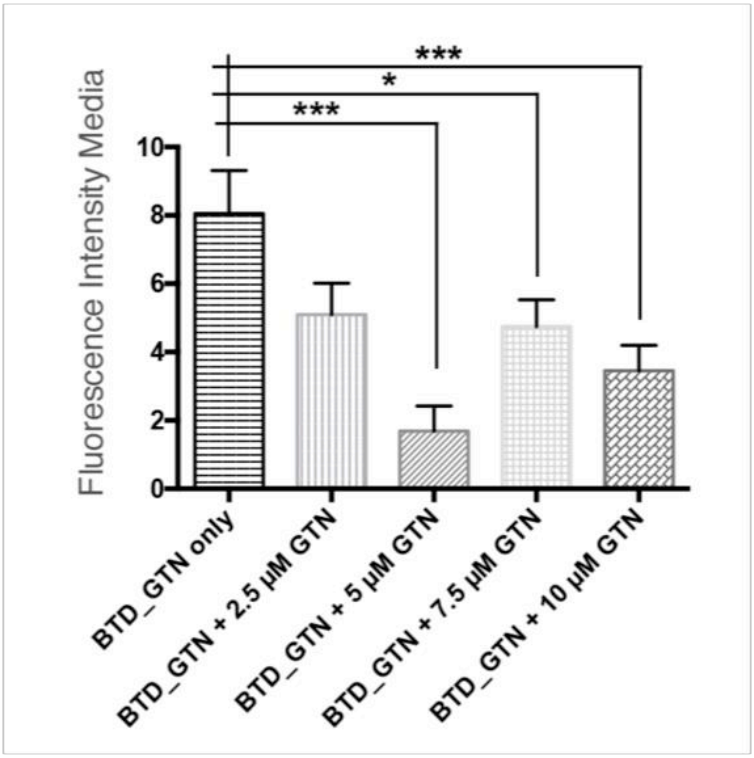

Figure S10. Quantitative analyses of fluorescence emission intensities from fluorescence dislodgee assay (GTN x BTD-GTN). The sample pre-incubated with GTN solution produces reduction of fluorescence emission intensities. Only the fluorescence emission reduction obtained from sample pre-incubated with GTN solution at 2.5 µM showed no statistic significance. * = $p \leq 0.05$ - *** = $p \leq 0.001$

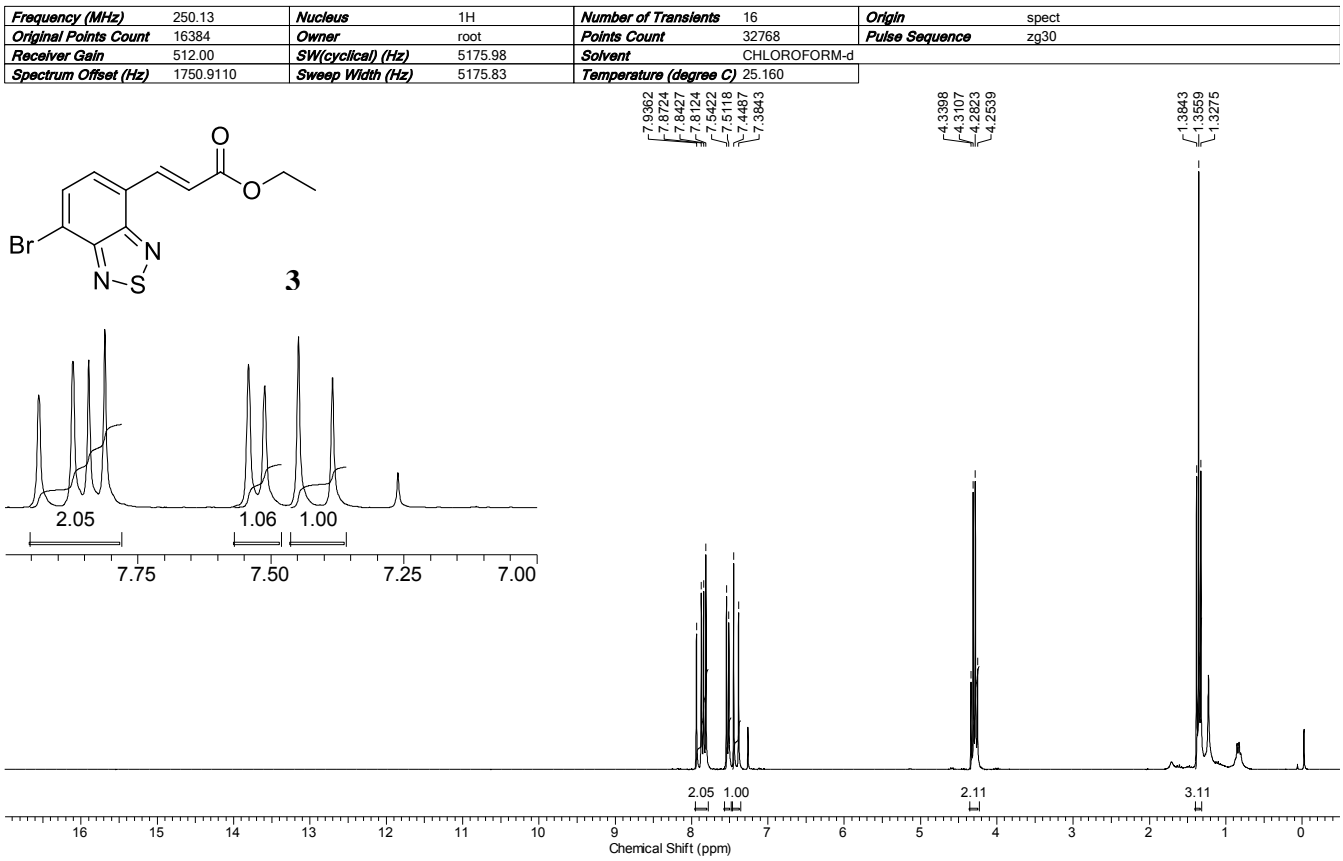

Figure S11: ^{1}H NMR spectrum (250 MHz, $CDCl_3$) for compound **3**.

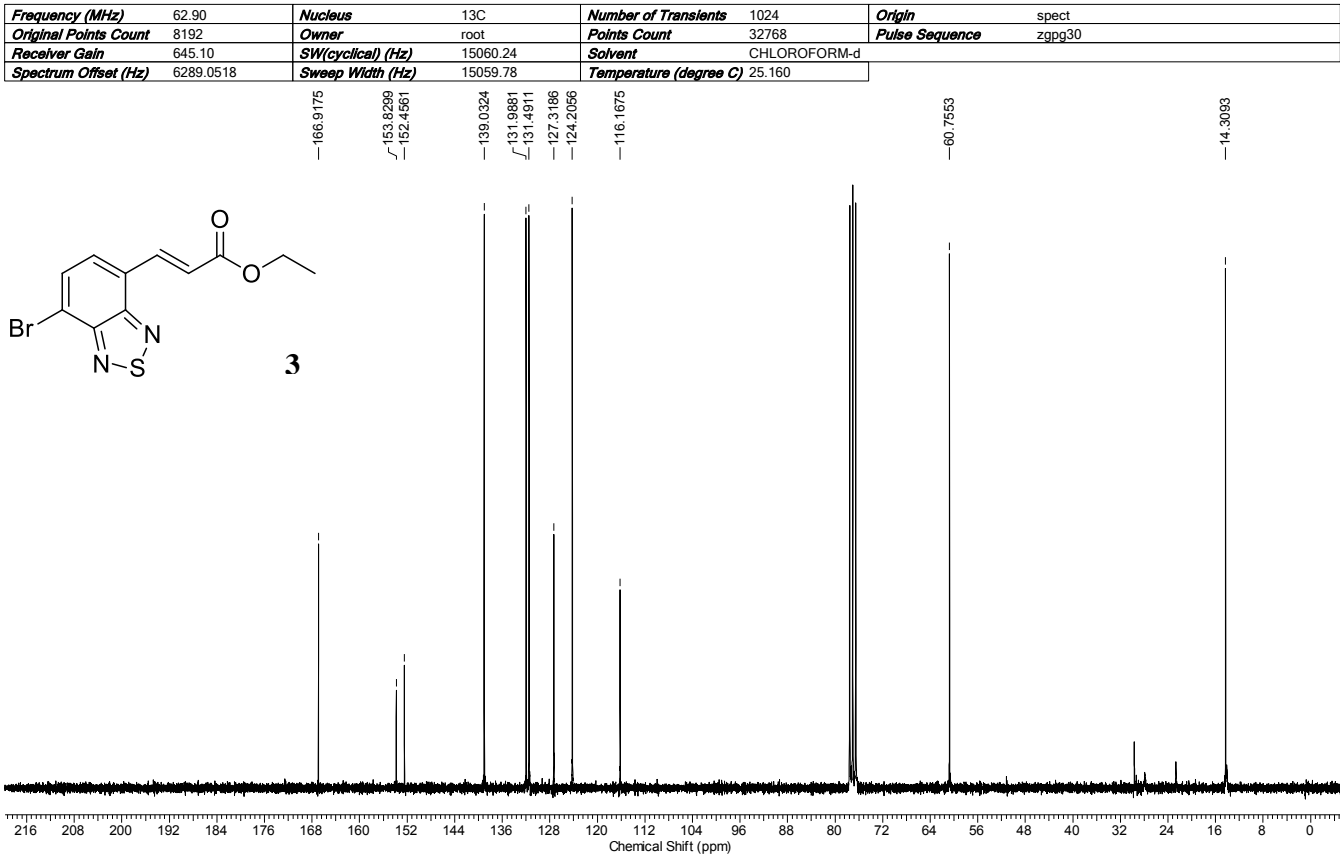

Figure S12: ^{13}C NMR spectrum (62,5 MHz, $CDCl_3$) for compound **3**.

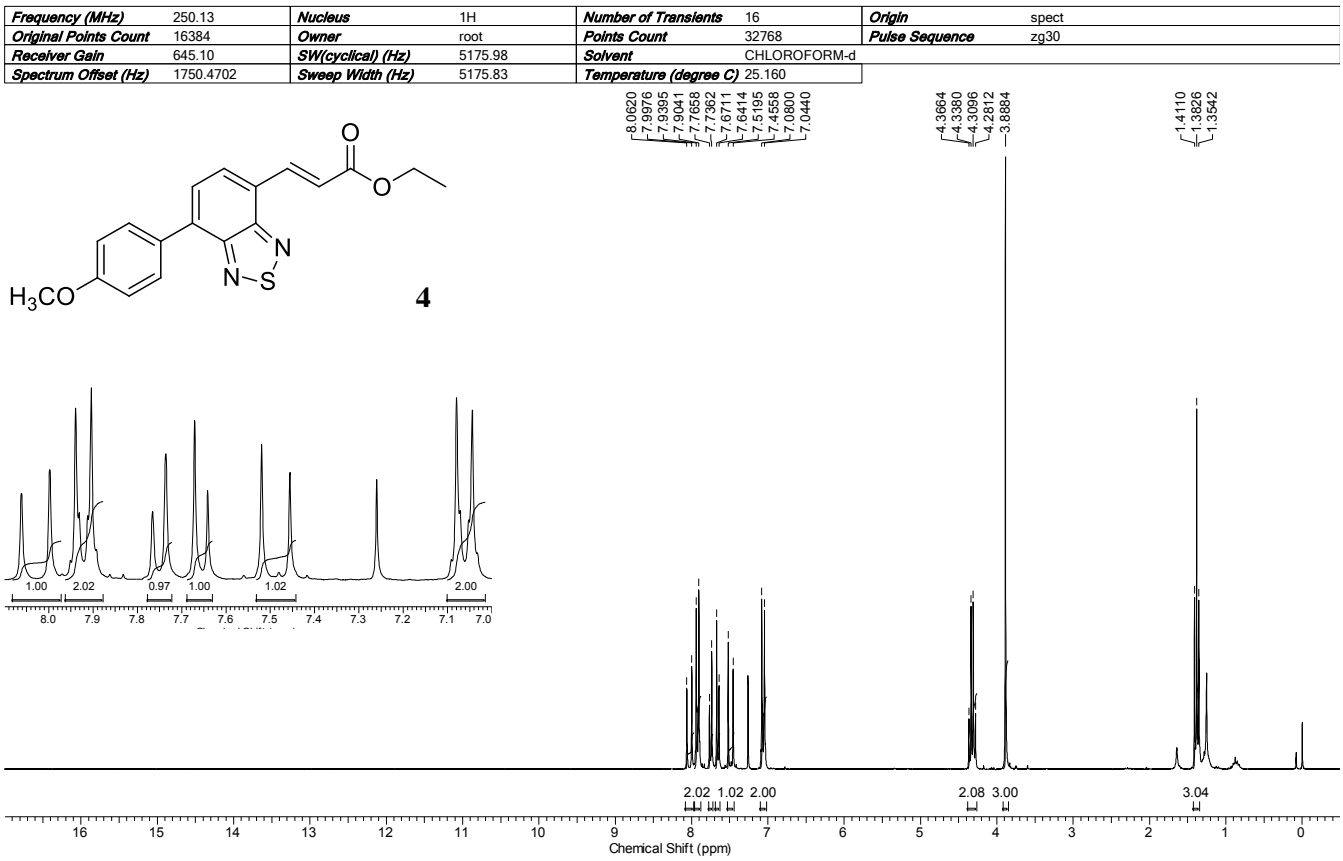

Figure S13: ^{1}H NMR spectrum (250 MHz, $CDCl_3$) for compound **4**.

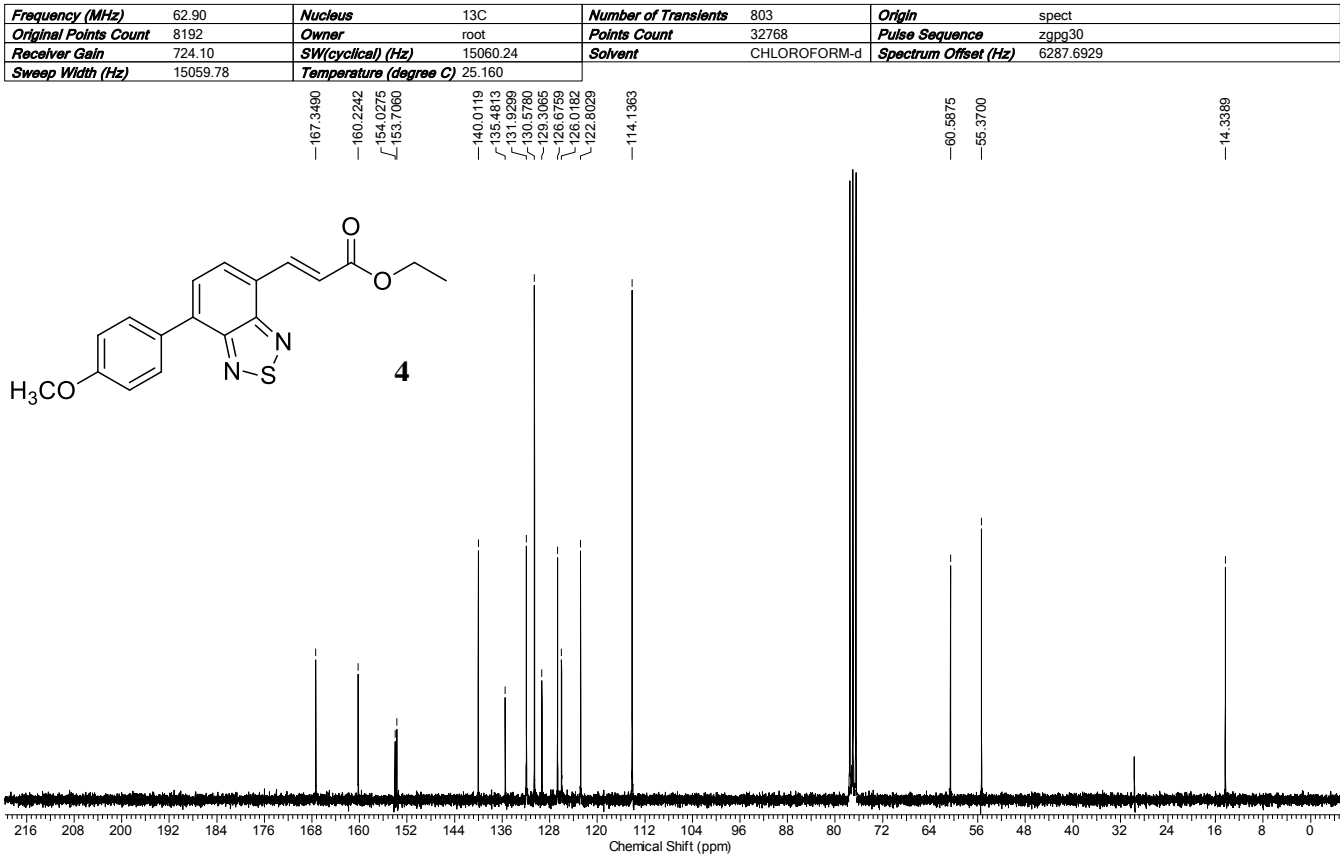

Figure S14: ^{13}C NMR spectrum (62,5 MHz, $CDCl_3$) for compound **4**.

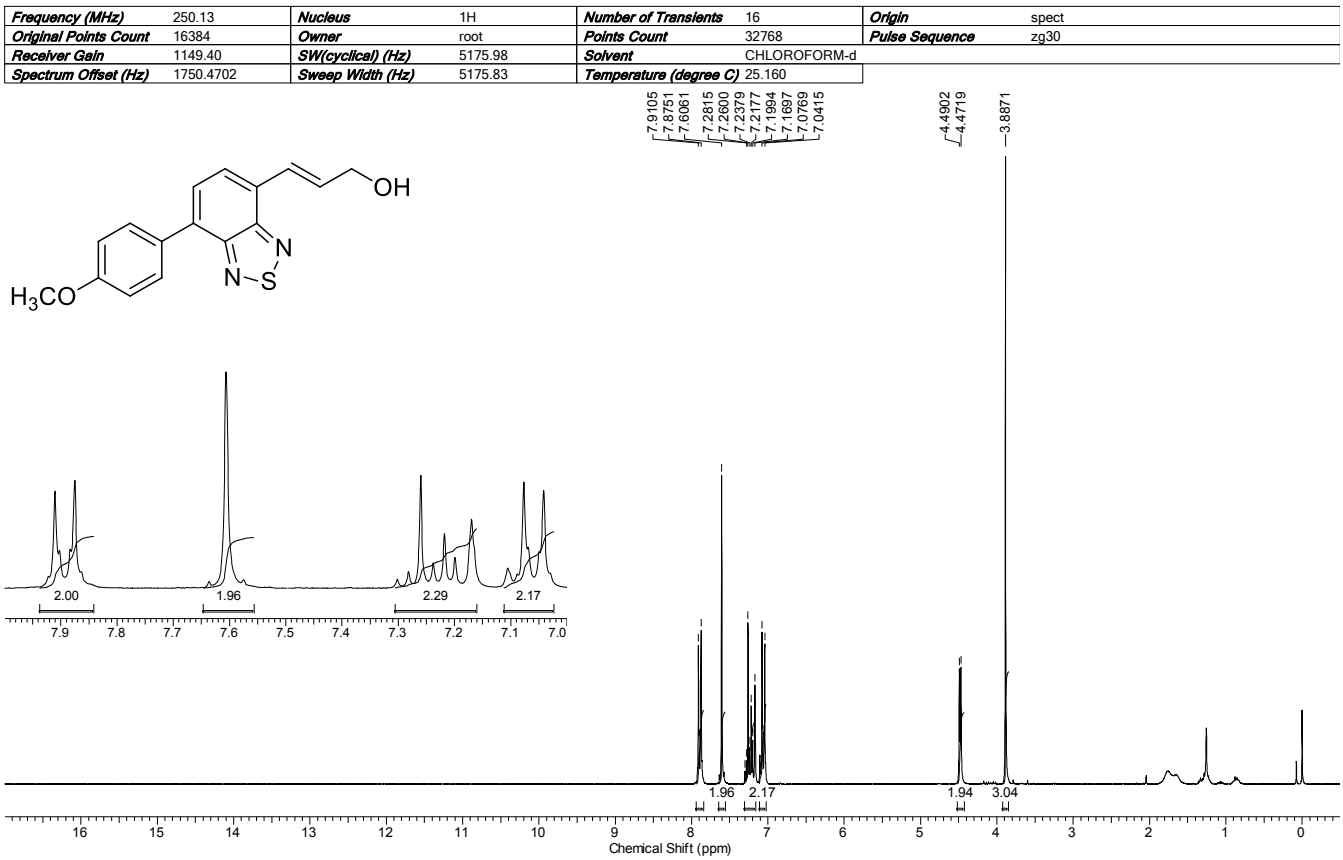

Figure S15: ^{1}H NMR spectrum (250 MHz, $CDCl_3$) for (*E*)-3-(7-(4-methoxyphenyl)benzo[c][1,2,5]thiadiazol-4-yl)prop-2-en-1-ol.

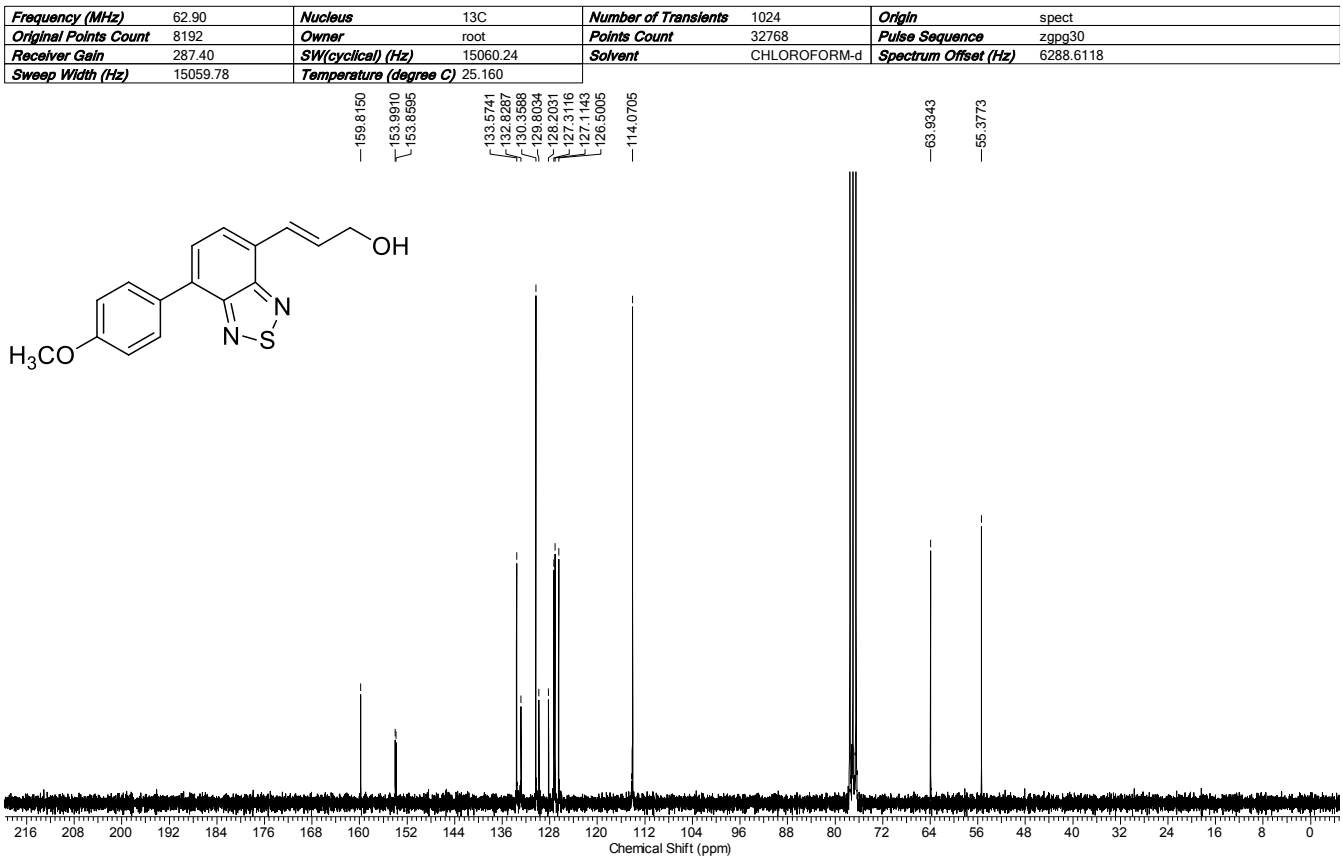

Figure S16: ^{13}C NMR spectrum (62,5 MHz, $CDCl_3$) for (*E*)-3-(7-(4-methoxyphenyl)benzo[c][1,2,5]thiadiazol-4-yl)prop-2-en-1-ol.

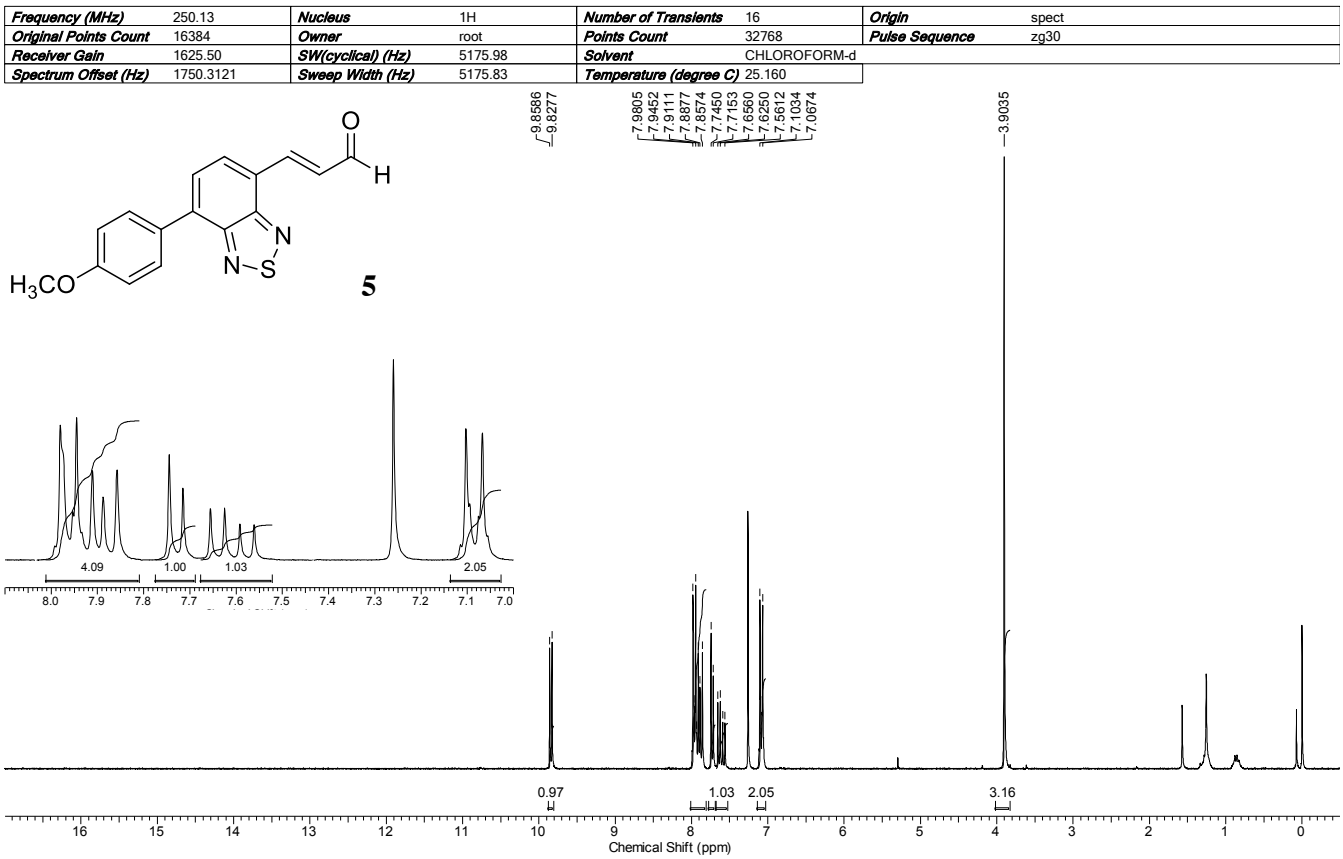

Figure S17: ^{1}H NMR spectrum (250 MHz, $CDCl_3$) for compound **5**.

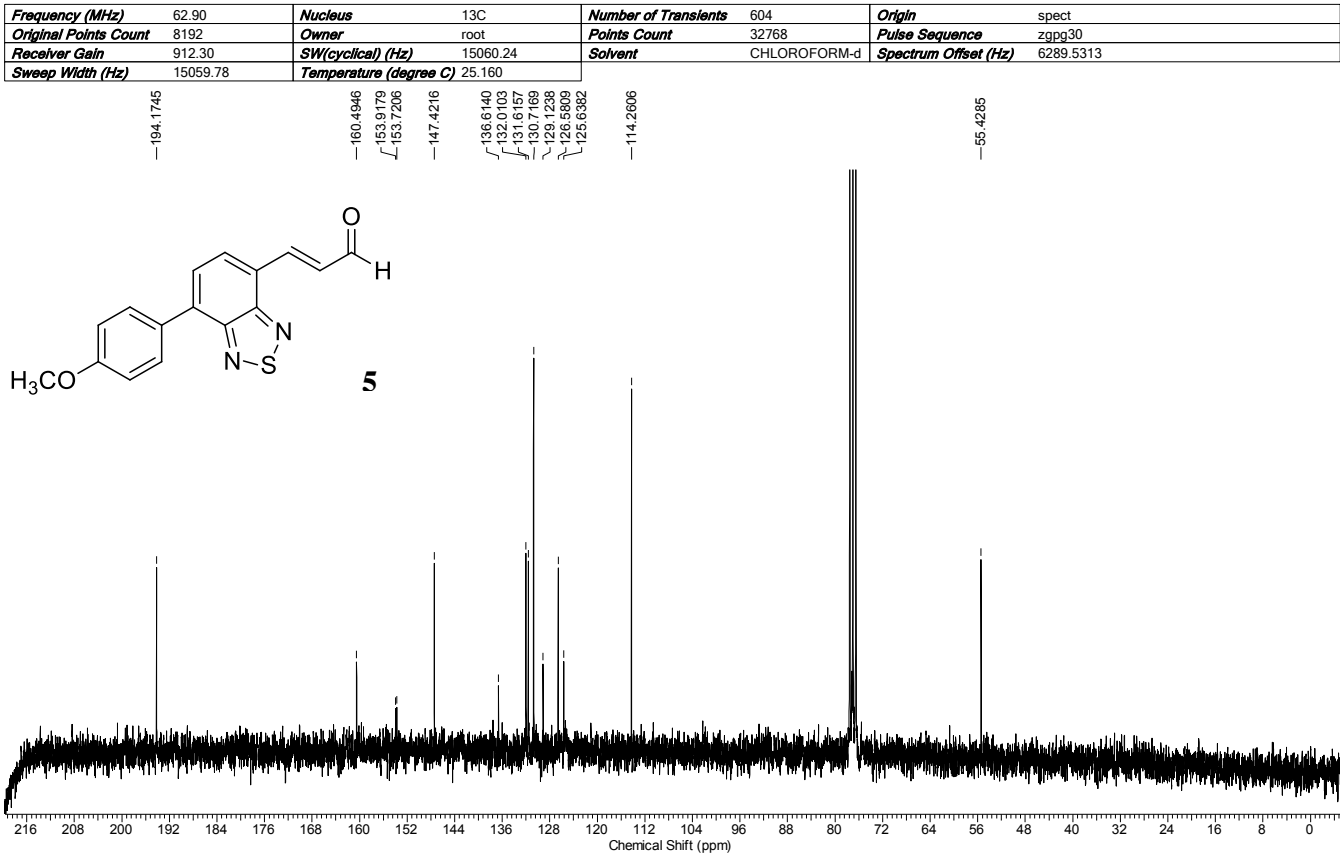

Figure S18: ^{13}C NMR spectrum (62,5 MHz, $CDCl_3$) for compound **5**.

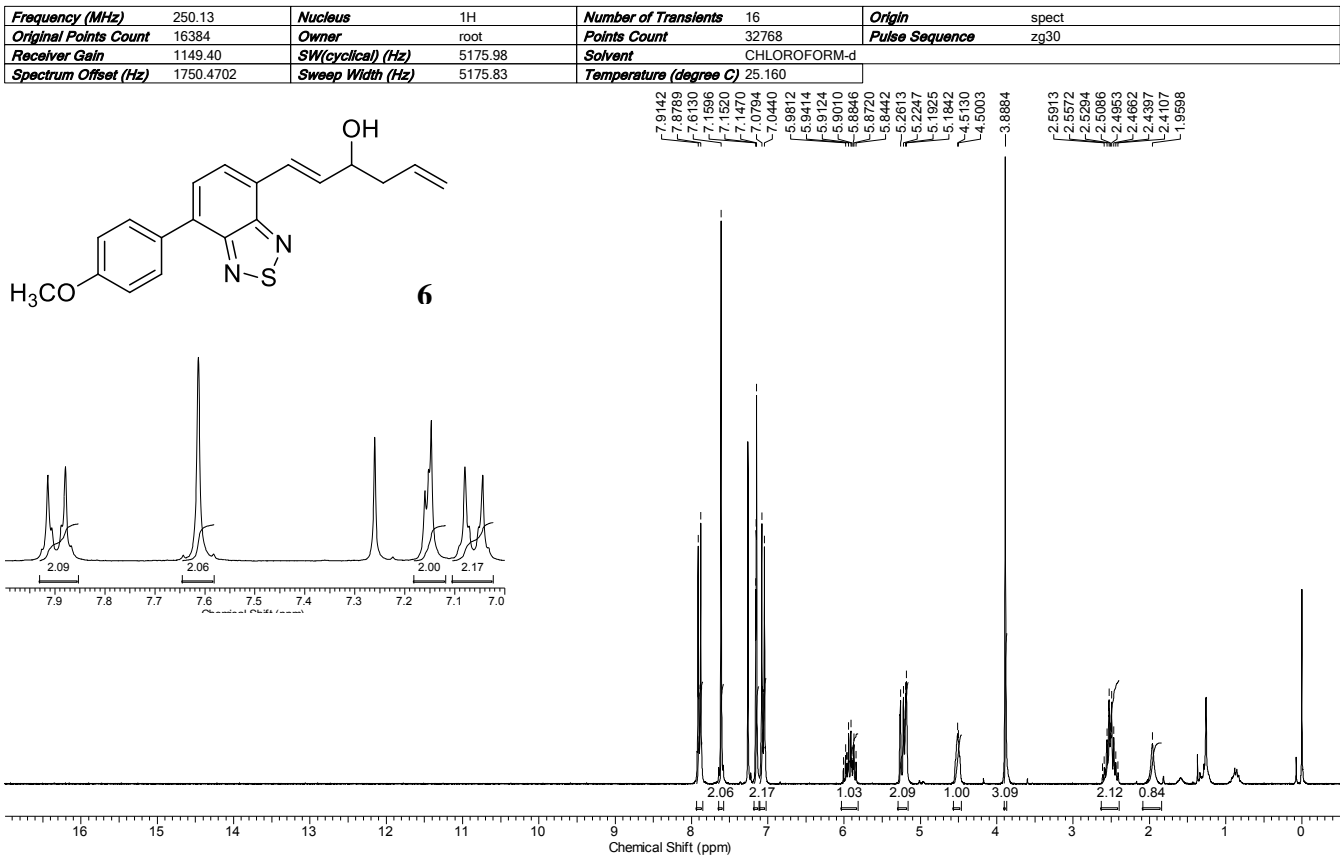

Figure S19: ^{1}H NMR spectrum (250 MHz, $CDCl_3$) for compound **6**.

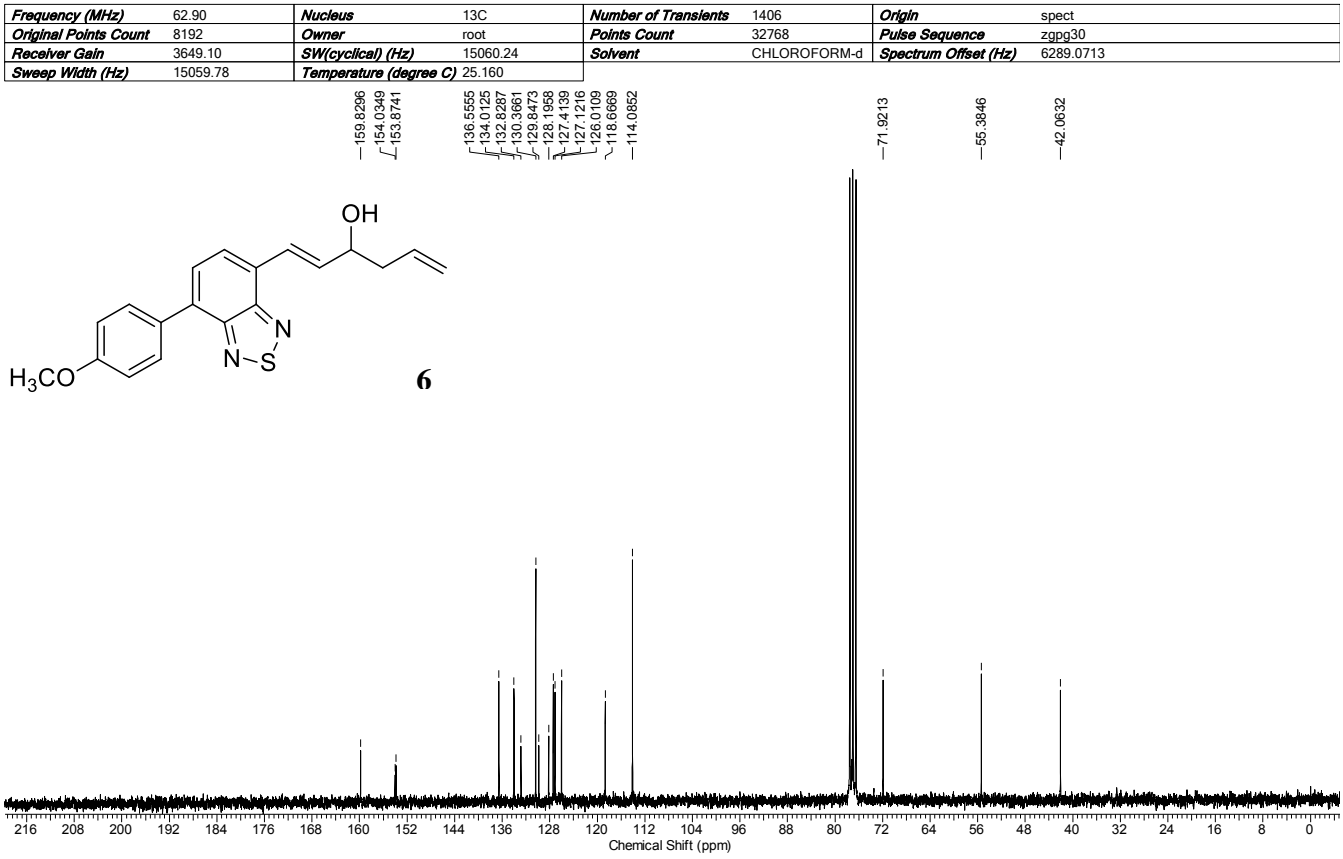

Figure S20: ^{13}C NMR spectrum (62,5 MHz, $CDCl_3$) for compound **6**.

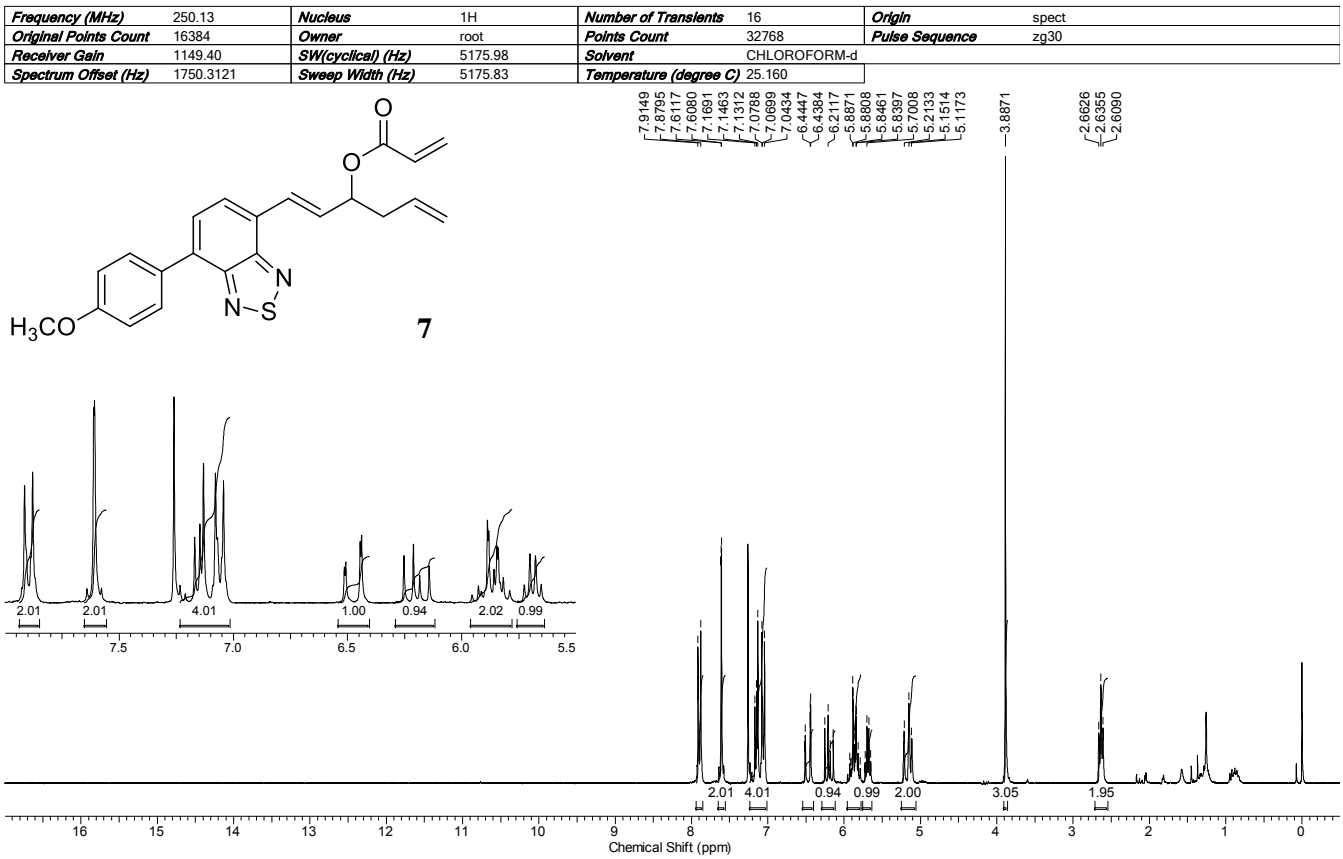

Figure S21: ^{1}H NMR spectrum (250 MHz, $CDCl_3$) for compound **7**.

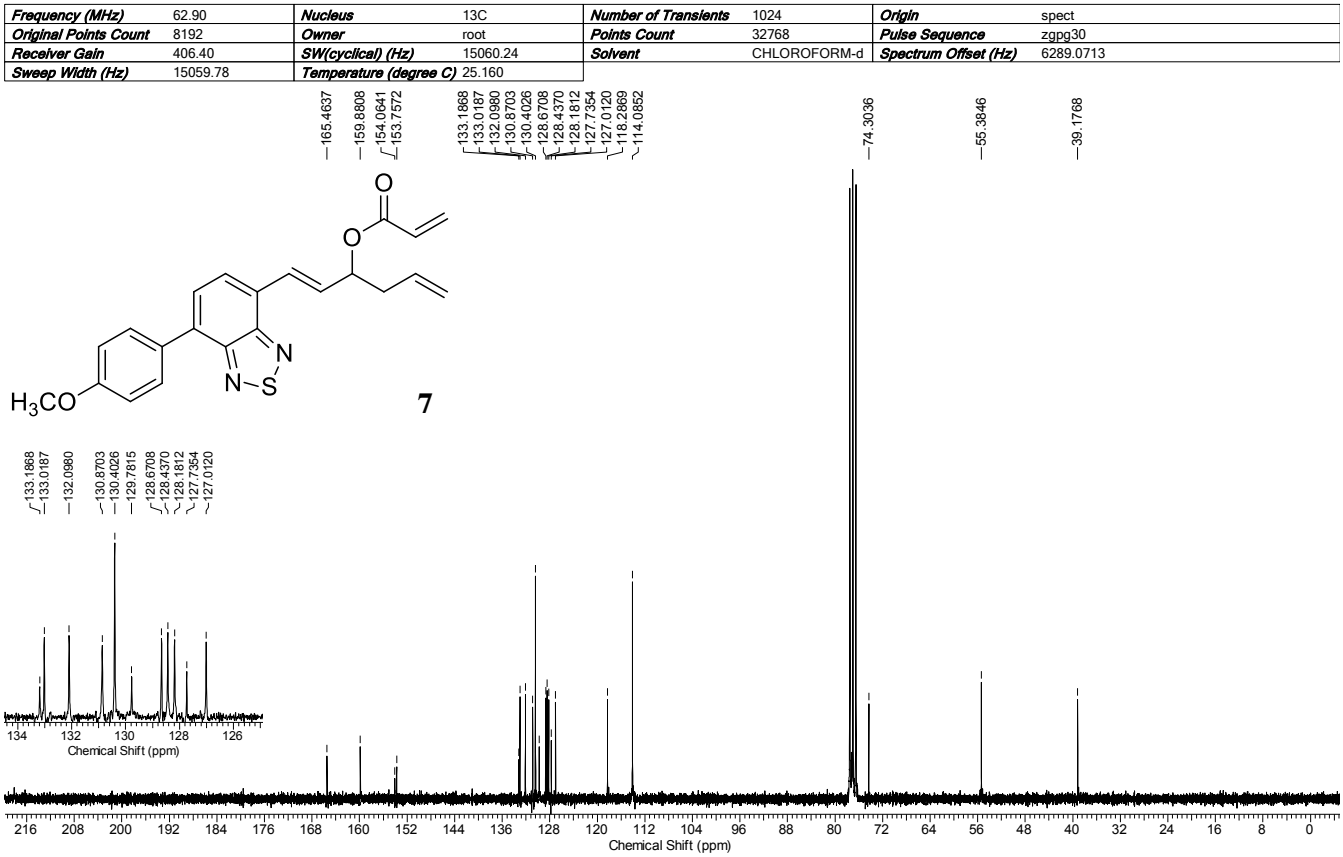

Figure S22: ^{13}C NMR spectrum (62,5 MHz, $CDCl_3$) for compound **7**.

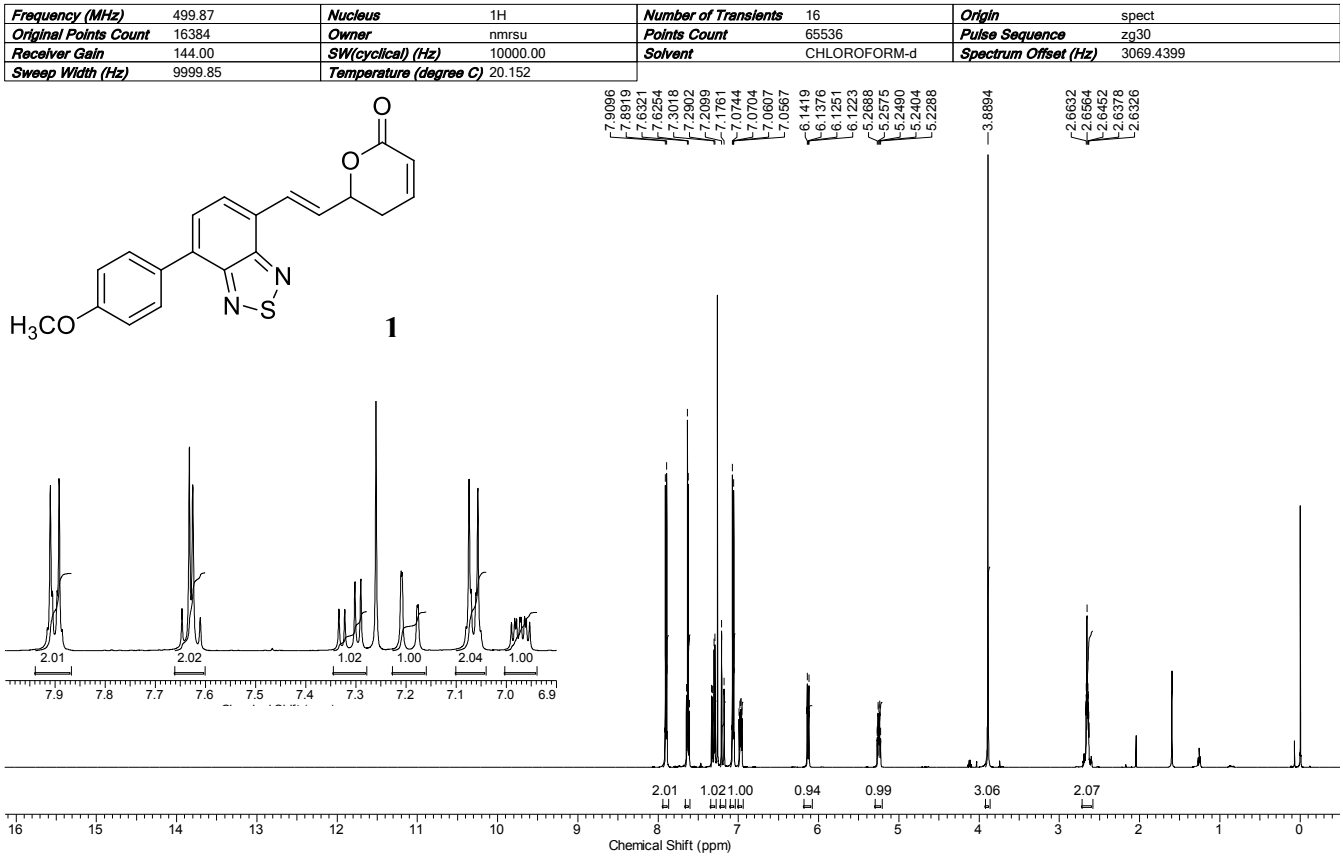

Figure S23: ^{1}H NMR spectrum (500 MHz, $CDCl_3$) for compound **1**.

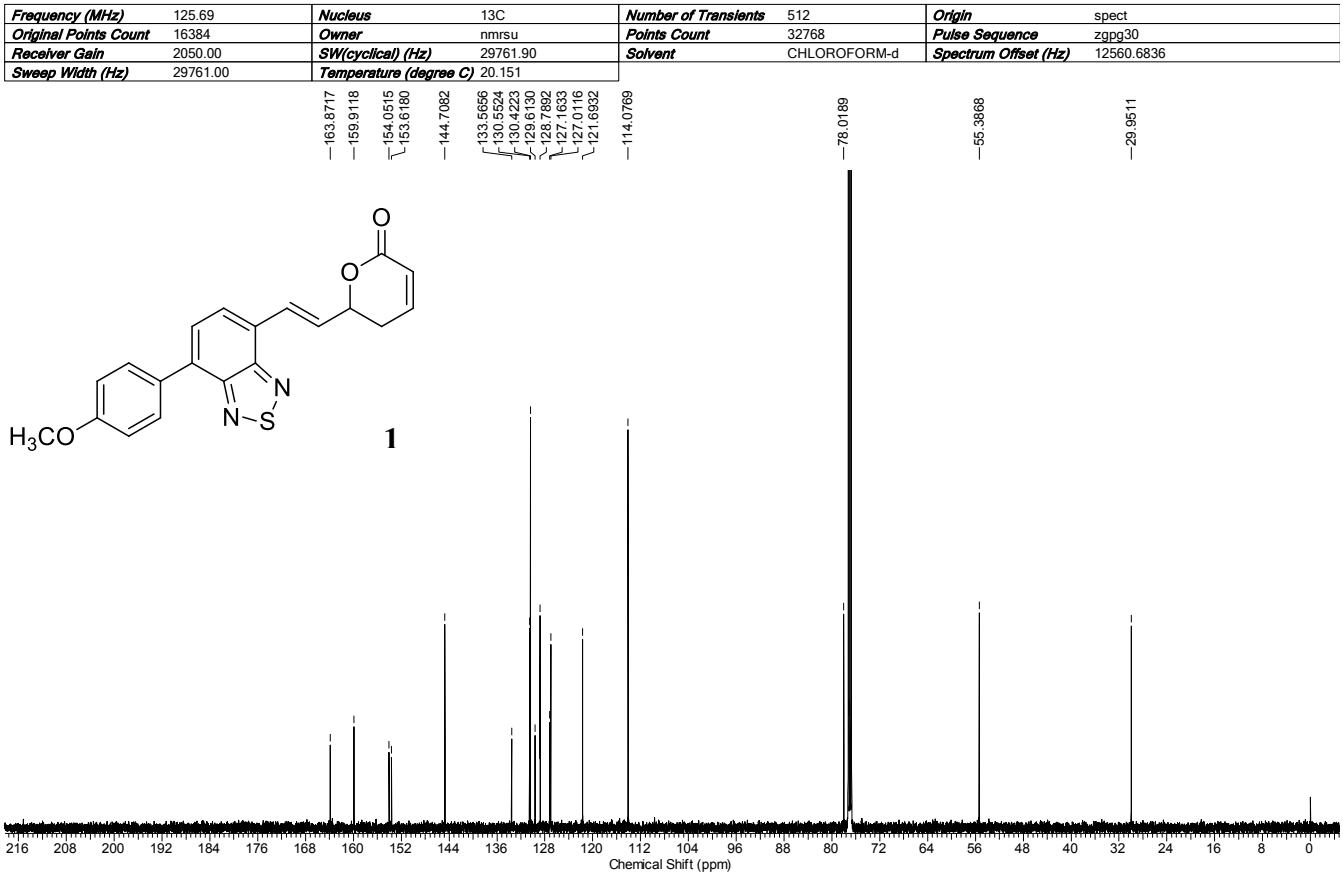

Figure S24: ^{13}C NMR spectrum (125 MHz, $CDCl_3$) for compound **1**.